Volume 99, Number 1, January–February 1994
Journal of Research of the National Institute of Standards and Technology

[J. Res. Natl. Inst. Stand. Technol. 99, 19 (1994)]

The NIST 30 MHz Linear Measurement System

Volume 99 Number 1 January–February 1994

Jeffrey A. Jargon, Ronald A. Ginley, and Douglas D. Sutton

National Institute of Standards and Technology,
Boulder, CO 80303-3328

An automated linear measurement system (LMS) has been developed to determine the nonlinearity of a tuned 30 MHz power detector over a 6.021 dB range. This detector uses a single thermistor bead design with thermal isolation to obtain nearly linear tracking over a 4:1 change in input power. The nonlinear correction for this change, determined by the LMS, is on the order of 1.00030 (+130 μB) for the detector presently in use. Initial experiments indicate an expanded uncertainty of ±0.138% (±598 μB), which is based upon Type A and Type B components.

Key words: attenuation; automated; calibration; linear; measurement; power; thermistor; uncertainty.

Accepted: November 16, 1993

1. Introduction

There has been a recent interest in and demand for a calibration service at NIST to support rf attenuators and voltage doublers that operate specifically at 30 MHz. The first step required to offer such a service is to develop a reference standard. For the best possible accuracy, a tuned single-element thermistor mount was chosen. A linear measurement system was designed and constructed at NIST to calibrate the nonlinearity of this mount. This paper contains a description of the LMS, an explanation of the measurement scheme, calibration results, and an uncertainty analysis.

2. System Description

A diagram of the system is shown in Fig. 1. The signal generator provides a stable 30 MHz rf signal that is amplified and filtered before the signal is split into two channels. One channel consists of a variable phase shifter and a fixed attenuator. A coaxial switch either terminates the signal with a 50 Ω termination or feeds the signal into a power divider, which splits the signal again. Half of the signal is detected by a single-element thermistor mount, P_1, and the other half is fed into the hybrid. The second channel consists of a variable attenuator. Like the first channel, a coaxial switch either terminates the signal with a 50 Ω load or feeds the signal into a power divider, which splits the signal. Half of the signal is detected by a single-element thermistor mount, P_2, and the other half is fed into the hybrid.

The hybrid takes the sum and difference of the two input signals. The difference is fed into a diode detector to rectify the signal, and then into a null meter. The sum is fed into a coaxial switch, and when the switch is in position 1, the signal is detected by a third thermistor mount, P_3, which is the thermistor to be calibrated.

Each thermistor mount is connected to a NIST Type IV bridge and a digital voltmeter to measure rf power.

The computer controls the signal generator, the digital voltmeters, and the switch controller, and handles the data acquisition and processing through an IEEE-488 bus.

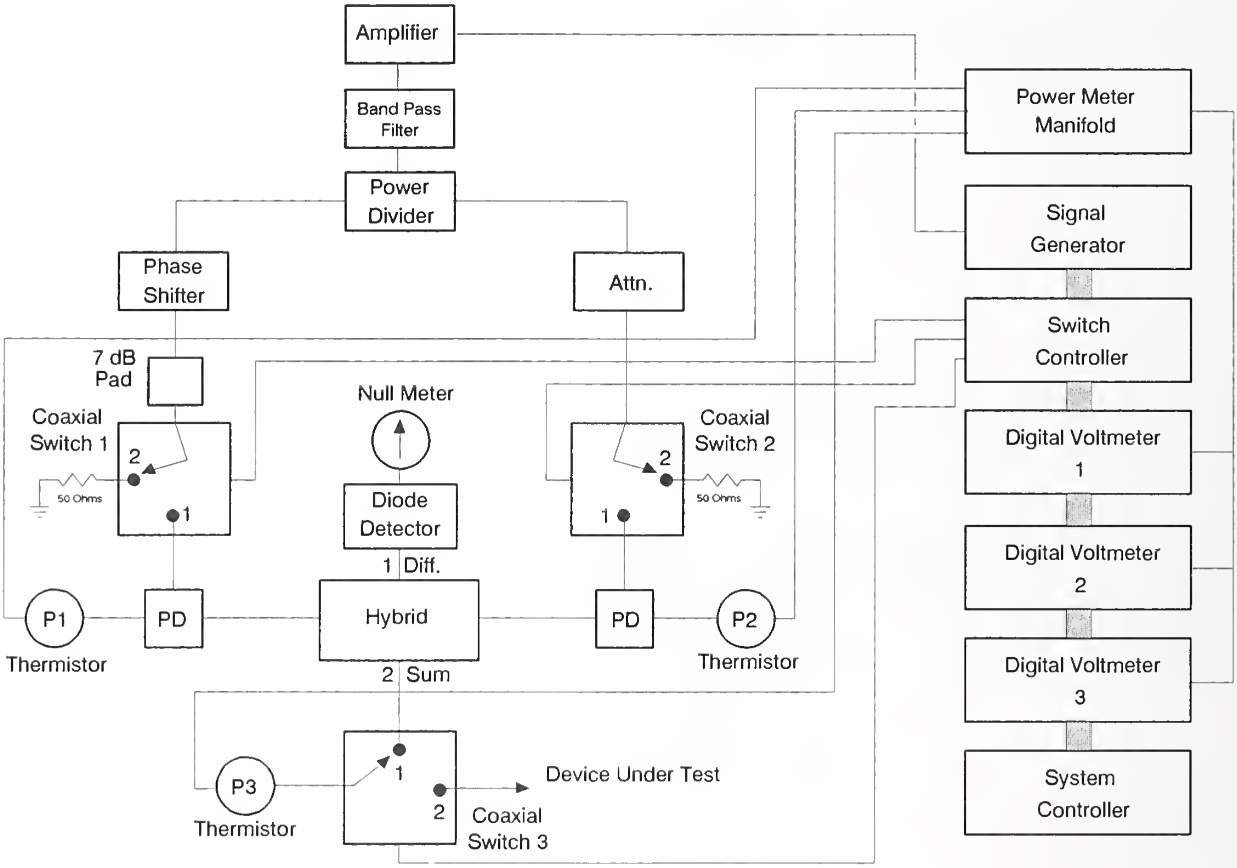

Fig. 1. Block diagram of 30 MHz linear measurement system.

3. Design of 30 MHz Single-Element Thermistor Mount

The dc response of detector P_3 must be nearly linear with changes in input rf power. A single 50 Ω thermistor bead design was selected as a linear detection scheme [1]. This detector is used in conjunction with a NIST Type IV self-balancing dc-substitution rf power meter modified to bias a 50 Ω detector [2]. The Type IV power meter is designed to change the thermistor bead bias current so that the thermistor always maintains the same resistance. The detectors are placed in the LMS housing where the temperature is held to ±0.2 °C.

It is difficult to filter the rf signal from the power meter leads due to the nature of the single bead. The total rf signal should appear across the bead in the ideal case. Other considerations in the detector design include thermal stability and any forms of rf leakage into or out of the detector.

Several ideas are incorporated in the detector to eliminate these problems. Figure 2 shows the circuit diagram of a single-element thermistor mount. LC filter sections are inserted to filter the rf signal in the power meter leads. No ferrite material (such as a ferrite core inductor) is used near the thermistor, since ferrite components experience changes in impedance with changes in the rf power. These impedance changes lead to nonlinearities in the detector response. Therefore, air-cored inductors are inserted near the thermistor. Ferrite-cored conductors are allowable in sections following the first filter section because the rf power is sufficiently reduced and renders any impedance variation negligible. The parallel LC filter is tuned to resonate at 30 MHz. A special thermistor-mounting structure has been developed, and consists of an electrically insulated doughnut and two copper blocks, one on either side of the doughnut. The thermistor is placed inside the doughnut hole and is encapsulated in an air pocket by the addition of the copper blocks. The copper blocks also provide a large thermal mass so that the entire structure cannot experience rapid changes in temperature. The thermal time constant is much longer than the time required to perform a single measurement cycle. Double-sided copper-clad fiberglass boards are used in the exterior detector housing and in the

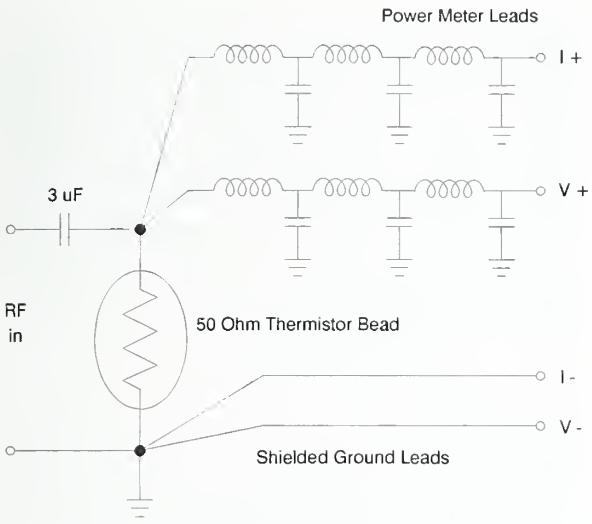

Fig. 2. Circuit diagram of single-element thermistor mount. All inductors are hand-wound and all capacitors are 1 μF unless otherwise labeled.

internal compartment walls which separate various filter sections. This type of construction and the use of capacitive feedthroughs in the compartment walls reduce the amount of rf leakage though the detector. These physical and electrical construction considerations provide a stable linear detector with low rf leakage.

4. Measurement Methods

4.1. Calibration of P_3

Three power meters are used in the LMS—P_1, P_2, and P_3. When a given power meter is read, the notation used is P_{XYZr}, where X denotes the power meter (1, 2, or 3), Y is 1 if channel 1 is switched on and 0 if channel 1 is switched off, Z is 1 if channel 2 is switched on and 0 if channel 2 is switched off, and "r" denotes that this power is a reading and not a true value. Powers without a subscript "r" are true values.

The calibration of P_3 is achieved using a three-stage method. First, with switches 1, 2, and 3 each in position 1, enough power is applied so that a nominal 12 mW is incident on the three thermistor mounts. The phase shifter and variable attenuator are adjusted to balance the two channels, thus obtaining a null on the null meter. Readings are taken on P_1, P_2, and P_3 and are designated P_{111r}, P_{211r}, and P_{311r}, respectively. Next, switch 2 is moved to position 2, so that power is only applied to the first channel. Readings are taken on P_1 and P_3 and are designated P_{110r} and P_{310r}, respectively. A nominal 12 mW will be incident on P_1 and approximately 3 mW will be incident on P_3. Finally, switch 2 is moved back to position 1 and switch 1 is moved to position 2, so that power is only applied to the second channel. Readings are taken on P_2 and P_3 and are designated P_{201r} and P_{301r}, respectively. A nominal 12 mW will be incident on P_2 and approximately 3 mW will be incident on P_3.

The calibration constant of P_3, denoted C_{HL}^2, is calculated using

$$C_{\mathrm{HL}}^2 = \left[\left(\frac{\dfrac{P_{310r}}{P_{110r}}}{\dfrac{P_{311r}}{P_{111r}}} \right)^{1/2} + \left(\frac{\dfrac{P_{301r}}{P_{201r}}}{\dfrac{P_{311r}}{P_{211r}}} \right)^{1/2} \right]^2 . \tag{1}$$

The derivation of this formula can be found in Appendix A. The calibration constant is a measure of the detector's nonlinearity over the 6.021 dB power change, and is used as a multiplication factor to correct the ratio measured by P_3, where

$$\frac{P_{311}}{P_{310}} = C_{\mathrm{HL}}^2 \frac{P_{311r}}{P_{310r}} . \tag{2}$$

4.2. Power Measurements

The NIST Type IV power meter must be connected to an external dc voltmeter. The substituted dc power, P_{dc}, is calculated from measured voltages using

$$P_{\mathrm{dc}} = \frac{V_{\mathrm{off}}^2 - V_{\mathrm{on}}^2}{R_0} , \tag{3}$$

where V_{off} is the output voltage with no rf power applied, V_{on} is the output voltage with rf applied, and R_0 (50 Ω) is the resistance of the thermistor mount. Figure 3 shows the measurement sequence for a power calculation [3]. An initial V_{off} is taken; rf power is applied and V_{on} is measured; rf power is removed and a final V_{off} is taken. The initial and final dc measurements are used with the V_{on} measurement to calculate the power and correct for any mount drift, which is assumed to be linear. The calculated value of V_{off} in Eq. (3) is given by

$$V_{\mathrm{off}} = V_{\mathrm{off,i}} + \frac{t_2 - t_1}{t_3 - t_1} (V_{\mathrm{off,f}} - V_{\mathrm{off,i}}) , \tag{4}$$

where $V_{\mathrm{off,i}}$ is the voltage reading taken before rf is applied at time t_1, $V_{\mathrm{off,f}}$ is the voltage taken after rf is removed at time t_3, and t_2 is the time at which V_{on} is taken.

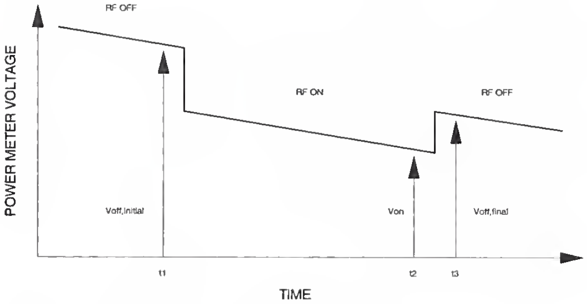

Fig. 3. Sequence for measuring power meter dc voltages.

5. Results

The calibration constant, C^2_{HL}, which is a measure of the nonlinearity of mount P_3, was obtained by repeated measurements. The average value of the three hundred trials taken so far is $C^2_{\mathrm{HL}} = 1.00030$ or $+130$ μB. Long-term data are being accumulated to validate the calibration of P_3.

Table 1 shows a sample calibration. Powers read by the three thermistor mounts are displayed for each of the three stages. The calculated calibration constant is shown, along with the actual step in power for each leg of the system.

Table 1. Sample calibration results of the 30 MHz Linear Measurement System's standard mount

	Switches 1&2	Switch 1	Switch 2
P(1)	11.5194	11.5089	0.0000
P(2)	11.4170	0.0001	11.3991
P(3)	11.0907	2.7644	2.7756

Leg 1: 6.0335 dB
Leg 2: 6.0160 dB

C^2_{HL} : 1.00029

6. Uncertainty Analysis

6.1. Evaluation of Type A Standard Uncertainty

Evaluation of a Type A standard uncertainty may be based on any valid statistical method for treating data. Examples are calculating the standard deviation of the mean of a series of independent observations, using the method of least squares to fit a curve to data in order to estimate the parameters of the curve and their standard deviations, and carrying out an analysis of variance in order to identify and quantify random effects in certain kinds of measurements [4].

The calibration of the standard mount, P_3, has been repeated three hundred times to determine the repeatability of the system. Tests were performed at various times of the day over several days to cover as many random factors as possible, including variations of environmental conditions and the operator's ability to renull the system. The sample standard deviation of the mean is $\pm 0.000335\%$ or ± 2 μB. Long-term data are being accumulated to validate this calibration, and a control chart is being developed to track any possible outliers or drift.

6.2. Evaluation of Type B Standard Uncertainty

Evaluation of a Type B standard uncertainty is based upon scientific judgment using all of the available relevant information. This includes previous measurement data, manufacturers' specifications, data provided in calibration reports, knowledge of the behavior of relevant instruments and materials, and uncertainties assigned to reference data taken from handbooks [4].

The Type B evaluation of standard uncertainty accounts for the following factors:

a. Uncertainty in the dc voltmeter measurements.
b. Uncertainty in the Type IV power meters.
c. Imperfect isolation between the two legs.
d. Uncertainty because $P_{301} \neq P_{310}$.
e. Effects of impedance changes in P_3.
f. RF leakage.
g. Spurious signals and harmonics.

6.2.1 Voltmeter Uncertainty The uncertainty in the individual voltmeter readings may be determined by taking the total differential of the power expression, Eq. (3), which gives

$$\mathrm{d}P = \frac{2}{R_0}\left(V_{\mathrm{off}}\,\mathrm{d}V_{\mathrm{off}} - V_{\mathrm{on}}\,\mathrm{d}V_{\mathrm{on}}\right) . \tag{5}$$

The total differential of power, Eq. (5), may be determined by taking the differential of V_{off}, Eq. (4), which gives

$$\mathrm{d}V_{\mathrm{off}} = (1-T)\mathrm{d}V_{\mathrm{off,i}} + T\mathrm{d}V_{\mathrm{off,f}} , \tag{6}$$

where

$$T = \frac{t_2 - t_1}{t_3 - t_1} . \tag{7}$$

The uncertainties, $\mathrm{d}V_{\mathrm{off,i}}$, $\mathrm{d}V_{\mathrm{off,f}}$, and $\mathrm{d}V_{\mathrm{on}}$, in the measured values of $V_{\mathrm{off,i}}$, $V_{\mathrm{off,f}}$, and V_{on}, are based on the voltmeter manufacturer's specifications.

Figure 4 shows the uncertainty in the power measurement as a function of power level, assuming the powers are ratioed as they are in the C^2_{HL}

calculation, Eq. (1). The power measurements, P_{301} and P_{310}, which are approximately 3 mW, result in uncertainties of 0.036%. The other power measurements, which are approximately 12 mW, result in uncertainties of 0.008%. The uncertainty of $C^2_{\rm HL}$ due to the voltmeter readings may be found by inserting the individual power uncertainties into Eq. (1), which gives

$$C^2_{\rm HL} + \Delta_v = \left[\left(\frac{\dfrac{P_{310}+\Delta_{310}}{P_{110}-\Delta_{110}}}{\dfrac{P_{311}+\Delta_{311}}{P_{111}-\Delta_{111}}} \right)^{1/2} + \left(\frac{\dfrac{P_{301}+\Delta_{301}}{P_{201}-\Delta_{201}}}{\dfrac{P_{311}+\Delta_{311}}{P_{211}-\Delta_{211}}} \right)^{1/2} \right]^2 . \qquad (8)$$

This results in an uncertainty of $\Delta_V = \pm 0.028\%$ or ± 122 μB.

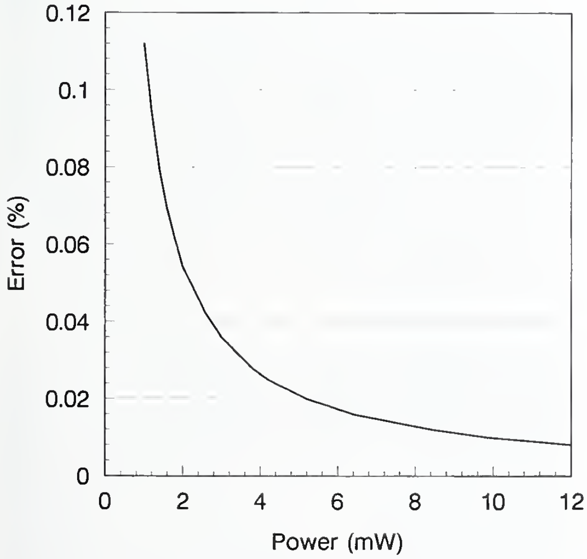

Fig. 4. Power measurement uncertainty due to DVM when ratios are taken.

6.2.2 Type IV Power-Meter Uncertainty The four possible sources of uncertainties internal to the Type IV power meter are the reference resistors, the operational amplifier open-loop gain, input offset voltage, and input bias current. Larsen has shown that the uncertainties due to the Type IV power meters are negligible compared to those of the voltmeters [2].

6.2.3 Imperfect Isolation An uncertainty in the calculation of $C^2_{\rm HL}$ may result if P_1 and P_2 are not zero when they are assumed to be. The thermistor mounts are square-law detectors and are not sufficiently sensitive to determine whether P_1 and P_2 are low enough in the "off" condition to avoid significant errors. This uncertainty is derived in Appendix B.

The corrected formula for $C^2_{\rm HL}$, taking imperfect isolation into account, is

$$C^2_{\rm HL} = \left[\left(\frac{\dfrac{P_{310\rm r}}{P_{110\rm r}}}{\dfrac{P_{311\rm r}}{P_{111\rm r}}} \right)^{1/2} \frac{1}{|1+\beta_1|} + \left(\frac{\dfrac{P_{301\rm r}}{P_{201\rm r}}}{\dfrac{P_{311\rm r}}{P_{211\rm r}}} \right)^{1/2} \frac{1}{|1+\gamma|} \right]^2 , \qquad (9)$$

where

$$\beta_1 = -\frac{Q_{12}\Delta b_2}{b_{110}} \qquad (10)$$

and

$$\gamma_1 = -\frac{\Delta b_1}{b_{201}Q_{12}} . \qquad (11)$$

Here, γ_1 is the measure of P_1's contribution to $C^2_{\rm HL}$ if it is not zero when it is assumed to be, and β_1 is the measure of P_2's contribution to $C^2_{\rm HL}$ if it is not zero when it is assumed to be. The terms, b_{110} and b_{201} are the corresponding voltages to the powers P_{110} and P_{201}, respectively. Assuming P_{110} and P_{201} are 12 mW, b_{110} and b_{201} are equal to 0.7746 V. The term, Q_{12}, is defined in Appendix B and its value is approximately -1. The Δb's represent the b's which were assumed to be zero in Appendix A. If the isolation between the channels is 65 dB, as is stated in the power divider manufacturer's specifications, then $\Delta b_1 = \Delta b_2 = 0.000436$. Using nominal values for the P's and substituting the values into Eq. (9), an uncertainty of $\pm 0.112\%$ or ± 488 μB is obtained.

6.2.4 Uncertainty Because $P_{301} \neq P_{310}$ An uncertainty in the calculation of $C^2_{\rm HL}$ may result if $P_{301} \neq P_{310}$. The derivation of this uncertainty can be found in Appendix C.

The measure of nonlinearity, α, of thermistor mount three is

$$\alpha = \frac{1 - C^2_{\rm HL}}{C^2_{\rm HL}\, P_{\rm Lr} - P_{\rm Hr}} , \qquad (12)$$

where P_{Lr} is the reading of mount three at the low level and P_{Hr} is the power reading of mount three at the high level. Assuming $C_{HL}^2 = 1.0004$ worst case, $P_{Lr} = 3$ mW, and $P_{Hr} = 12$ mW, α is calculated to be 3.334×10^{-5}. The ratio K_{301}/K_{310} is given by

$$\frac{K_{301}}{K_{310}} = \frac{1 + \alpha P_{301r}}{1 + \alpha P_{310r}} . \qquad (13)$$

If P_{301r} is 10% greater than P_{310r}, then

$$\frac{K_{301}}{K_{310}} = \frac{1 + \alpha(3 \times 1.10)}{1 + \alpha(3)} = 1.000010. \qquad (14)$$

The effect of this being nonunity results in a corrected formula for C_{HL}^2, where

$$C_{HL}^2 = \left[\left(\frac{\dfrac{P_{310r}}{P_{110r}}}{\dfrac{P_{311r}}{P_{111r}}} \right)^{1/2} + \left(\frac{\dfrac{K_{301}}{K_{310}} \dfrac{P_{310r}}{P_{201r}}}{\dfrac{P_{311r}}{P_{211r}}} \right)^{1/2} \right]^2$$

$$= 1.000005 \qquad (15)$$

using nominal values for the P's. The result is an uncertainty of ±0.0005% or ±3 μB.

6.2.5 Uncertainty Due to Impedance Changes in P_3 An uncertainty in the calculation of C_{HL}^2 may result if the impedance changes in P_3 with power level. The derivation of this uncertainty can be found in Appendix D.

The corrected formula for C_{HL}^2, taking impedance changes in P_3 into account, is

$$C_{HL}^2 = \frac{\left[\left(\dfrac{\dfrac{P_{310r}}{P_{110r}}}{\dfrac{P_{311r}}{P_{111r}}} \right)^{1/2} + \left(\dfrac{\dfrac{P_{301r}}{P_{201r}}}{\dfrac{P_{311r}}{P_{211r}}} \right)^{1/2} \right]^2}{\left| \dfrac{1 - \Gamma_{LMS}\,\Gamma_{311}}{1 - \Gamma_{LMS}\,\Gamma_{310}} \right|^2 \dfrac{(1 - |\Gamma_{310}|^2)}{(1 - |\Gamma_{311}|^2)}} , \qquad (16)$$

where Γ_{311} is the reflection coefficient of mount three at the high level, Γ_{310} is the reflection coefficient of mount three at the low level, and Γ_{LMS} is the reflection coefficient of the system looking into port three.

The measured value of Γ_{310} was actually taken 10 dB below Γ_{310} instead of the 6 dB step, so the uncertainty should be conservative. Using nominal values for the P's and the measured reflection coefficients, the calculated uncertainty is ±0.014% or ±62 μB.

Impedance changes in the diode detector with respect to power level are assumed to have a negligible effect on the overall uncertainty.

6.2.6 Uncertainty Due to RF Leakage It is difficult to assign a quantitative uncertainty due to rf leakage. In order to reduce leakage, all coaxial cables in the system were replaced with semirigid lines and, wherever possible, SMA connectors were used. For now, the uncertainty due to rf leakage is assumed to be ±10 μB or ±0.0023%.

6.2.7 Uncertainty Due to Spurious Signals and Harmonics After the signal is amplified and filtered, any harmonics are at least −92 dBc, while spurious signals are no greater than −84 dBc. This will result in a measurement error that will affect the uncertainty of C_{HL}^2.

From Eq. (3), the calculated dc power is

$$P_{dc} = 20\ (V_{off}^2 - V_{on}^2), \qquad (17)$$

where P_{dc} is in mW. Assuming $V_{off} = 1$ V, then $V_{on} = 0.63246$ V for a calculated power of 12 mW and $V_{on} = 0.92195$ V for a calculated power of 3 mW.

A harmonic at −92 dBc results in an uncertainty of ±0.0025% for a voltage measurement. This uncertainty translates to power uncertainties of (12±0.0004) mW and (3±0.0008) mW. Using the nominal powers to calculate C_{HL}^2, an uncertainty of ±0.023% or ±100 μB is obtained.

A spurious signal at −112 dBc results in an uncertainty of ±0.00025% for a voltage measurement. This uncertainty translates to power uncertainties of (12±0.00004) mW and (3±0.000085) mW. Using the nominal powers to calculate C_{HL}^2, an uncertainty of ±0.0025% or ±11 μB is obtained.

6.2.8. Overall Type B Uncertainty For each Type B component, an estimated range, $\pm a_j$, is given, assuming that the quantity in question has a 100% probability of lying within that interval. The quantity is treated as if it is equally probable for its value to lie anywhere within the interval. Therefore, it is modeled by a rectangular probability distribution. The best estimate of the standard deviation, u_j, is

$$u_j = \frac{a_j}{\sqrt{3}} . \qquad (18)$$

Table 2 shows all of the Type B components along with their corresponding uncertainties and standard deviations. The overall standard deviation of the Type B components, calculated using the root-sum-of-squares method (RSS), is ±0.069% or ±299 μB.

Table 2. Type B components of the 30 MHz Linear Measurement System with corresponding uncertainty ranges and standard deviations

Component	Range (%)	Standard deviation (%)
dc voltage measurements	±0.028	0.016
Imperfect isolation	±0.112	0.065
$P_{301} \neq P_{310}$	±0.0005	0.0003
Impedance changes in P_3	±0.014	0.008
rf leakage	±0.0023	0.0013
Spurious signals	±0.0025	0.0014
Harmonics	±0.023	0.013
Combined Type B Standard Uncertainty (RSS)		± 0.069 (±299 μB)

6.3 Combined Standard Uncertainty

The combined standard uncertainty, u_c, is taken to represent the estimated standard deviation of the result. It is obtained by combining the individual standard deviations, u_i, whether arising from a Type A or a Type B evaluation [4]. The technique used to combine the standard deviations is the RSS method.

The total uncertainty reported is the expanded uncertainty, U, which is obtained by multiplying u_c by a coverage factor, k. To be consistent with current international practice, the value of k used at NIST for calculating U is $k=2$. The total expanded uncertainty, U, of the mount's nonlinearity is calculated to be ±0.138% or ±598 μB.

7. Conclusion

The first step toward offering a calibration service at NIST to support rf attenuators and voltage doublers that operate at 30 MHz has been completed. The reference standard, a tuned single-element thermistor mount, has been calibrated using an LMS, designed and constructed at NIST. The next step is to modify the LMS so that a device under test may be inserted into the system and calibrated against the reference standard.

8. Appendix A. Scattering Coefficient Analysis of the LMS

The 30 MHz Linear Measurement System can be considered a five port network, as shown in Fig. 5. The analysis assumes that the LMS is an ideal system—that is, the system is linear, and when b_1 and b_2 are assumed to be 0, they truly are.

The pertinent scattering coefficients are

$$\begin{aligned}
b_1 &= S_{11}a_1 + S_{12}a_2 + S_{13}a_3 + S_{14}a_4 + S_{15}a_5 \\
b_2 &= S_{21}a_1 + S_{22}a_2 + S_{23}a_3 + S_{24}a_4 + S_{25}a_5 \\
b_3 &= S_{31}a_1 + S_{32}a_2 + S_{33}a_3 + S_{34}a_4 + S_{35}a_5 \\
b_4 &= S_{41}a_1 + S_{42}a_2 + S_{43}a_3 + S_{44}a_4 + S_{45}a_5 \\
b_5 &= S_{51}a_1 + S_{52}a_2 + S_{53}a_3 + S_{54}a_4 + S_{55}a_5 .
\end{aligned} \tag{19}$$

If $a_1 = \Gamma_1 b_1$ and $a_2 = \Gamma_2 b_2$, then Eq. (19) may be written as

$$\begin{aligned}
b_1(1-\Gamma_1 S_{11}) &= S_{12}\Gamma_2 b_2 + S_{13}a_3 + S_{14}a_4 + S_{15}a_5 \\
b_2(1-\Gamma_2 S_{22}) &= S_{21}\Gamma_1 b_1 + S_{23}a_3 + S_{24}a_4 + S_{25}a_5 \\
b_3 &= S_{31}\Gamma_1 b_1 + S_{32}\Gamma_2 b_2 + S_{33}a_3 + S_{34}a_4 + S_{35}a_5 \\
b_4 &= S_{41}\Gamma_1 b_1 + S_{42}\Gamma_2 b_2 + S_{43}a_3 + S_{44}a_4 + S_{45}a_5 \\
b_5 &= S_{51}\Gamma_1 b_1 + S_{52}\Gamma_2 b_2 + S_{53}a_3 + S_{54}a_4 + S_{55}a_5
\end{aligned} \tag{20}$$

This gives five equations and eight unknown variables—a_3, a_4, a_5, b_1, b_2, b_3, b_4, and b_5. Four variables can be eliminated from Eq. (20), say a_4, b_4, a_5, and b_5. Eq. (20) becomes

$$b_1 = P'_{13}a_3 + Q'_{12}\, b_2 + Q'_{13}b_3 \; , \tag{21}$$

where the primed quantities are functions of the scattering coefficients and Γ_1 and Γ_2.

It is assumed that Γ_3 is constant with respect to varying power levels. If now $a_3 = \Gamma_3 b_3$,

$$\begin{aligned}
b_1 = (P'_{13}\,\Gamma_3 + Q'_{13})b_3 + Q'_{12}b_2 \equiv \\
Q_{13}b_3 + Q_{12}b_2
\end{aligned} \tag{22}$$

or

$$b_3 = \frac{b_1 - Q_{12}b_2}{Q_{13}} \; , \tag{23}$$

where two complex constants, Q_{12} and Q_{13}, describe the relationship among b_1, b_2, and b_3.

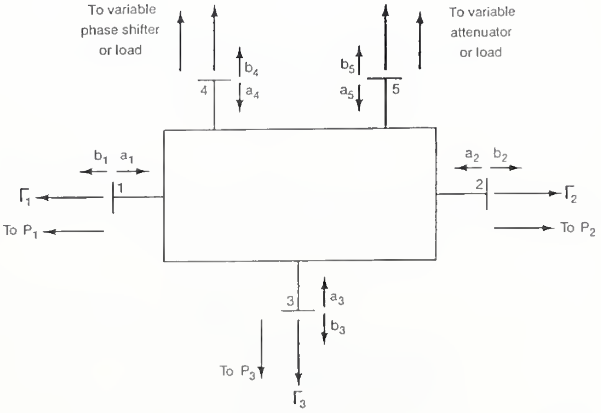

Fig. 5. LMS port nomenclature.

Equation (23) may be applied under three conditions: subscript "10" when $b_2=0$; "01" when $b_1=0$; and "11" when neither b_1 nor b_2 equal 0. Thus

$$b_{311}=\frac{b_{111}-Q_{12}b_{211}}{Q_{13}}, \tag{24}$$

where b_{311} is the value of b_3 when b_1 and b_2 are both energized from ports four and five. When $b_2=0$, which occurs by energizing port four and terminating port five, Eq. (23) becomes

$$b_{310}=\frac{b_{110}}{Q_{13}} \tag{25}$$

or

$$Q_{13}=\frac{\mathrm{b}_{110}}{\mathrm{b}_{310}}\,. \tag{26}$$

Similarly, when $b_1=0$, which occurs by energizing port five and terminating port four, Eq. (23) becomes

$$b_{301}=\frac{-Q_{12}}{Q_{13}}\,b_{201}\,. \tag{27}$$

Substituting Eq. (26) into Eq. (27) gives

$$b_{301}=\ -Q_{12}b_{201}\,\frac{b_{310}}{b_{110}} \tag{28}$$

or

$$-Q_{12}=\frac{b_{301}}{b_{201}}\frac{b_{110}}{b_{310}}\,. \tag{29}$$

Substituting Eqs. (26) and (29) into Eq. (24) gives

$$1=\frac{b_{111}}{b_{311}}\frac{b_{310}}{b_{110}}+\frac{b_{211}}{b_{311}}\frac{b_{301}}{b_{201}}\,. \tag{30}$$

The b's are complex numbers. If the phase is measured relative to b_{111}/b_{311}, then

$$\begin{split}1=\frac{b_{111}}{b_{311}}\left|\frac{b_{310}}{b_{110}}\right|e^{j\,\theta_{3110}}+{}\\ \left|\frac{b_{211}}{b_{311}}\right|e^{j\,\theta_{2311}}\left|\frac{b_{301}}{b_{201}}\right|\mathrm{e}^{j\,\theta_{3201}}.\end{split} \tag{31}$$

If $\theta=\theta_{2311}+\theta_{3201}-\theta_{3110}$, Eq. (31) becomes

$$\begin{split}1=e^{j}\,\theta_{3110}\left[\frac{b_{111}}{b_{311}}\left|\frac{b_{310}}{b_{110}}\right|+\right.\\ \left.\left|\frac{b_{211}}{b_{311}}\right|\left|\frac{b_{301}}{b_{201}}\right|e^{j\,\theta}\right].\end{split} \tag{32}$$

Since the detectors measure only magnitudes, the magnitude squared of Eq. (32) is

$$\begin{split}1=\left(\left|\frac{\dfrac{b_{310}}{b_{110}}}{\dfrac{b_{311}}{b_{111}}}\right|+\left|\frac{\dfrac{b_{301}}{b_{201}}}{\dfrac{b_{311}}{b_{211}}}\right|\cos\theta\right)^2+{}\\ \left|\frac{\dfrac{b_{301}}{b_{201}}}{\dfrac{b_{311}}{b_{211}}}\right|^2\sin^2\theta\,,\end{split} \tag{33}$$

which can also be written as

$$\begin{split}1=\left|\frac{\dfrac{b_{310}}{b_{110}}}{\dfrac{b_{311}}{b_{111}}}\right|^2+\left|\frac{\dfrac{b_{301}}{b_{201}}}{\dfrac{b_{311}}{b_{211}}}\right|^2+{}\\ 2\left|\frac{\dfrac{b_{310}}{b_{110}}}{\dfrac{b_{311}}{b_{111}}}\right|\left|\frac{\dfrac{b_{301}}{b_{201}}}{\dfrac{b_{311}}{b_{211}}}\right|\cos\theta\,.\end{split} \tag{34}$$

Since the powers are proportional to the squares of the voltages, Eq. (34) becomes

$$1=\frac{\dfrac{P_{310}}{P_{110}}}{\dfrac{P_{311}}{P_{111}}}+\frac{\dfrac{P_{301}}{P_{201}}}{\dfrac{P_{311}}{P_{211}}}+2\sqrt{\frac{\dfrac{P_{310}}{P_{110}}}{\dfrac{P_{311}}{P_{111}}}\ \frac{\dfrac{P_{301}}{P_{201}}}{\dfrac{P_{311}}{P_{211}}}}\ \cos\theta. \tag{35}$$

Completing the square and transposing terms gives

$$\begin{split}\left[\left(\frac{\dfrac{P_{310}}{P_{110}}}{\dfrac{P_{311}}{P_{111}}}\right)^{1/2}+\left(\frac{\dfrac{P_{301}}{P_{201}}}{\dfrac{P_{311}}{P_{211}}}\right)^{1/2}\right]^2=1+2\\ \sqrt{\frac{\dfrac{P_{310}}{P_{110}}}{\dfrac{P_{311}}{P_{111}}}\ \frac{\dfrac{P_{301}}{P_{201}}}{\dfrac{P_{301}}{P_{211}}}}\ (1-\cos\,\theta).\end{split} \tag{36}$$

Since the powers are all positive and $(1-\cos\theta)$ is greater than or equal to 0, the quantity on the left side of Eq. (36) is a minimum when a null is obtained ($\theta=0$). Since $\cos\theta$ approaches 1 as θ approaches 0, Eq. (36) becomes

$$1=\left[\left(\frac{\frac{P_{310}}{P_{110}}}{\frac{P_{311}}{P_{111}}}\right)^{1/2}+\left(\frac{\frac{P_{301}}{P_{201}}}{\frac{P_{311}}{P_{211}}}\right)^{1/2}\right]^2 . \qquad (37)$$

The above P's are the true powers. The detectors, however, give readings proportional to the true values. Furthermore, P_3 could have a different proportionality constant for the two levels if the detector is nonlinear. The ratio of these two proportionality constants is the desired result.

If the subscript "r" represents proportional readings, and the nonsubscripted P's represent the true values, then

$$\begin{aligned} P_1&=K_1\,P_{1r}\\ P_2&=K_2\,P_{2r}\\ P_{311}&=K_{311}\,P_{311r}\\ P_{310}&=K_{310}\,P_{310r}\\ P_{301}&=K_{301}\,P_{301r} \end{aligned} \qquad (38)$$

The powers, P_{310} and P_{301}, will ordinarily be very close, and essentially

$$K_{310}=K_{301} \qquad (39)$$

since the detectors are assumed to be very nearly linear. P_1 and P_2 remain essentially constant. Substituting Eqs. (38) and (39) into Eq. (37) gives

$$1=\left(\left(\frac{K_{310}}{K_{311}}\right)^{1/2}\left[\left(\frac{\frac{P_{310r}}{P_{110r}}}{\frac{P_{311r}}{P_{111r}}}\right)^{1/2}+\left(\frac{\frac{P_{301r}}{P_{201r}}}{\frac{P_{311r}}{P_{211r}}}\right)^{1/2}\right]\right)^2 \qquad (40)$$

or

$$C_{\mathrm{HL}}^2=\frac{K_{311}}{K_{310}}=\left[\left(\frac{\frac{P_{310r}}{P_{110r}}}{\frac{P_{311r}}{P_{111r}}}\right)^{1/2}+\left(\frac{\frac{P_{301r}}{P_{201r}}}{\frac{P_{311r}}{P_{211r}}}\right)^{1/2}\right]^2 , \qquad (41)$$

where C_{HL}^2 is the calibration constant that one must multiply the P_{311r}/P_{310r} reading by to get the true ratio

$$\frac{P_{311}}{P_{311}}=C_{\mathrm{HL}}^2\frac{P_{311r}}{P_{310r}} . \qquad (42)$$

The calibration constant should be used only when P_3 is operating at the two levels for which it was calibrated.

9. Appendix B. Imperfect Isolation

It is desirable to have an estimate of the error when P_1 and P_2 are not 0 when they are assumed to be. The detectors are square-law detectors and are not sufficiently sensitive to determine whether P_1 and P_2 are low enough in the "off" condition to avoid significant errors.

Let Δb's represent the b's which were assumed to be 0 in Appendix A. Equation (24) is still valid, but Eq. (25) should now be

$$b_{310}=\frac{b_{110}-Q_{12}\Delta b_2}{Q_{13}}=\frac{b_{110}}{Q_{13}}\left(1-\frac{Q_{12}\,\Delta b_2}{b_{110}}\right) \qquad (43)$$

and Eq. (27) should now be

$$b_{301}=\frac{\Delta b_1-Q_{12}\,b_{201}}{Q_{13}}=-\frac{Q_{12}b_{201}}{Q_{13}}\left(1-\frac{\Delta b_1}{b_{201}\,Q_{12}}\right). \qquad (44)$$

Let

$$\beta_1=-\frac{Q_{12}\,\Delta b_2}{b_{110}} \qquad (45)$$

and

$$\gamma_1=-\frac{\Delta b_1}{b_{201}Q_{12}} . \qquad (46)$$

Combining Eqs. (43)–(46) gives

$$Q_{13}=\frac{b_{110}}{b_{310}}(1+\beta_1) \qquad (47)$$

and

$$-Q_{12}=\frac{b_{301}}{b_{201}}\frac{b_{110}}{b_{310}}\frac{1+\beta_1}{1+\gamma_1} . \qquad (48)$$

Eq. (24) now becomes

$$1=\frac{\dfrac{b_{111}}{b_{311}}+\dfrac{b_{211}}{b_{311}}\dfrac{b_{301}}{b_{201}}\dfrac{b_{110}}{b_{310}}\dfrac{1+\beta_1}{1+\gamma_1}}{\dfrac{b_{110}}{b_{310}}(1+\beta_1)} \qquad (49)$$

or

$$1=\frac{b_{111}}{b_{311}}\frac{b_{310}}{b_{110}}\frac{1}{1+\beta_1}+\frac{b_{211}}{b_{311}}\frac{b_{301}}{b_{201}}\frac{1}{1+\gamma_1}\,. \tag{50}$$

The b's and β_1 and γ_1 are complex numbers. If the phase is measured relative to b_{111}/b_{311}, then

$$1=\frac{b_{111}}{b_{311}}\left|\frac{b_{310}}{b_{110}}\right|\frac{e^{j(\theta_{3110}-\theta_{\beta_1})}}{|1+\beta_1|}+\left|\frac{b_{211}}{b_{311}}\right|e^{j\theta_{2311}}$$

$$\left|\frac{b_{301}}{b_{201}}\right|\frac{e^{j(\theta_{3201}-\theta_{\gamma 1})}}{|1+\gamma_1|}\,, \tag{51}$$

where

$$\theta_{\beta_1}=Arg\ (1+\beta_1) \tag{52}$$

and

$$\theta_{\gamma_1}=Arg\ (1+\gamma_1)\,. \tag{53}$$

Equation (51) may also be written as

$$1=e^{j(\theta_{3110}-\theta_{\beta_1})}\left[\frac{\dfrac{|b_{310}|}{|b_{110}|}}{\dfrac{b_{311}}{b_{111}}|1+\beta_1|}+\right.$$

$$\left.\frac{\left|\dfrac{b_{301}}{b_{201}}\right|e^{j(\theta+\theta_{\beta_1}-\theta_{\gamma_1})}}{\left|\dfrac{b_{311}}{b_{211}}\right||1+\gamma_1|}\right], \tag{54}$$

where

$$\theta=\theta_{2311}+\theta_{3201}-\theta_{3110}. \tag{55}$$

As in Appendix A, taking the square of the magnitude and changing to power gives

$$1=\frac{\dfrac{P_{310}}{P_{110}}}{\dfrac{P_{311}}{P_{111}}|1+\beta_1|^2}+\frac{\dfrac{P_{301}}{P_{201}}}{\dfrac{P_{311}}{P_{211}}|1+\gamma_1|^2}+$$

$$P_{sq}\cos(\theta+\theta_{\beta_1}-\theta_{\gamma_1}), \tag{56}$$

where

$$P_{sq}=2\sqrt{\frac{\dfrac{P_{310}\,P_{301}}{P_{110}\,P_{201}}}{\dfrac{P_{311}\,P_{311}}{P_{111}\,P_{211}}|1+\beta_1|^2\,|1+\gamma_1|^2}}\,. \tag{57}$$

Completing the square of Eq. (56) and transposing terms gives

$$\left[\left(\frac{\dfrac{P_{310}}{P_{110}}}{\dfrac{P_{311}}{P_{111}}}\right)^{1/2}\frac{1}{|1+\beta_1|}+\left(\frac{\dfrac{P_{301}}{P_{201}}}{\dfrac{P_{311}}{P_{211}}}\right)^{1/2}\frac{1}{|1+\gamma_1|}\right)^2=$$

$$1+P_{sq}\left[1-\cos(\theta+\theta_{\beta_1}-\theta_{\gamma_1})\right]. \tag{58}$$

As in Appendix A, using the argument on the function being minimum when the angle is 0, and substituting in the proportional readings

$$C^2_{\mathrm{HL}}=\left[\left(\frac{\dfrac{P_{310\mathrm{r}}}{P_{110\mathrm{r}}}}{\dfrac{P_{311\mathrm{r}}}{P_{111\mathrm{r}}}}\right)^{1/2}\frac{1}{|1+\beta_1|}+\right.$$

$$\left.\left(\frac{\dfrac{P_{301\mathrm{r}}}{P_{201\mathrm{r}}}}{\dfrac{P_{311\mathrm{r}}}{P_{211\mathrm{r}}}}\right)^{1/2}\frac{1}{|1+\gamma_1|}\right]^2. \tag{59}$$

10. Appendix C. Error Due to $P_{301}\neq P_{310}$

Since the detectors are very close to being precisely linear, it is reasonable to model the nonlinearity by

$$P=KP_{\mathrm{r}}\,(1+\alpha P_{\mathrm{r}}),$$

where α is a measure of the nonlinearity. The nonsubscripted P is the true value and P_{r} is the proportional reading. Substituting Eq. (60) into Eq. (42)

$$\frac{P_{\mathrm{H}}}{P_{\mathrm{L}}}=C^2_{\mathrm{HL}}\frac{P_{\mathrm{Hr}}}{P_{\mathrm{Lr}}}=\frac{KP_{\mathrm{Hr}}\,(1+\alpha P_{\mathrm{Hr}})}{KP_{\mathrm{Lr}}\,(1+\alpha P_{\mathrm{Lr}})} \tag{61}$$

or

$$C^2_{\mathrm{HL}}=\frac{1+\alpha P_{\mathrm{Hr}}}{1+\alpha P_{\mathrm{Lr}}}\,. \tag{62}$$

Solving for α

$$\alpha=\frac{1-C^2_{\mathrm{HL}}}{C^2_{\mathrm{HL}}\,P_{\mathrm{Lr}}-P_{\mathrm{Hr}}} \tag{63}$$

The ratio K_{301}/K_{310} may be found using Eq. (60)

$$\frac{P_{301}}{P_{310}}=\frac{K_{301}P_{301\mathrm{r}}}{K_{310}P_{301\mathrm{r}}}=\frac{KP_{301\mathrm{r}}\,(1+\alpha P_{301\mathrm{r}})}{KP_{310\mathrm{r}}\,(1+\alpha P_{310\mathrm{r}})} \tag{64}$$

or

$$\frac{K_{301}}{K_{310}}=\frac{1+\alpha P_{301\mathrm{r}}}{1+\alpha P_{310\mathrm{r}}}\ . \tag{65}$$

The effect of this non-unity is obtained by substituting Eq. (38) and (65) into Eq. (37), which gives

$$1=\left(\left(\frac{K_{310}}{K_{311}}\right)^{1/2}\left[\left(\frac{\dfrac{P_{310\mathrm{r}}}{P_{110\mathrm{r}}}}{\dfrac{P_{311\mathrm{r}}}{P_{111\mathrm{r}}}}\right)^{1/2}+\left(\frac{\dfrac{K_{301}}{K_{310}}\dfrac{P_{301\mathrm{r}}}{P_{201\mathrm{r}}}}{\dfrac{P_{311\mathrm{r}}}{P_{211\mathrm{r}}}}\right)^{1/2}\right]\right)^2 \tag{66}$$

or

$$C_{\mathrm{HL}}^2=\frac{K_{311}}{K_{310}}=\left[\left(\frac{\dfrac{P_{310\mathrm{r}}}{P_{110\mathrm{r}}}}{\dfrac{P_{311\mathrm{r}}}{P_{111\mathrm{r}}}}\right)^{1/2}+\left(\frac{\dfrac{K_{301}}{K_{310}}\dfrac{P_{301\mathrm{r}}}{P_{201\mathrm{r}}}}{\dfrac{P_{311\mathrm{r}}}{P_{211\mathrm{r}}}}\right)^{1/2}\right]^2 . \tag{67}$$

11. Appendix D. Effects of Impedance Changes in P_3

Starting with Eq. (21),

$$b_1=P'_{13}a_3+Q'_{12}\,b_2+Q'_{13}b_3. \tag{68}$$

If ports four and five are terminated in impedances that null the hybrid, b_1 and b_2 are almost 0 even when a_3 is energized since the two legs of each power divider are isolated. Thus

$$\Gamma_{\mathrm{LMS}}=\frac{b_3}{a_3}\approx-\frac{P'_{13}}{Q'_{13}}\,, \tag{69}$$

where Γ_{LMS} is the reflection coefficient looking into port three when ports four and five are terminated with matching impedances. The second part of Eq. (69) is obtained from setting b_1 and b_2 to 0 in Eq. (68).

Substituting Eq. (69) into Eq. (68), and using $a_3=\Gamma_3\,b_3$ yields

$$b_1=Q'_{12}\,b_2+(-\Gamma_{\mathrm{LMS}}\,Q'_{13}\,\Gamma_3+Q'_{13})\,b_3 \tag{70}$$

or

$$b_3(1-\Gamma_{\mathrm{LMS}}\,\Gamma_3)=\frac{b_1}{Q'_{13}}-\frac{b_2Q'_{12}}{Q'_{13}}\ . \tag{71}$$

As before, making b_1 and b_2 successively 0, gives

$$Q'_{13}=\frac{b_{110}}{b_{310}}\,\frac{1}{1-\Gamma_{\mathrm{LMS}}\Gamma_{310}}\,. \tag{72}$$

and

$$-\frac{Q'_{12}}{Q'_{13}}=\frac{b_{301}}{b_{201}}\,(1-\Gamma_{\mathrm{LMS}}\,\Gamma_{301}). \tag{73}$$

Assuming $\Gamma_{310}=\Gamma_{301}$, since $b_{310}\approx b_{301}$, gives

$$-\frac{Q'_{12}}{Q'_{13}}=\frac{b_{301}}{b_{201}}\,(1-\Gamma_{\mathrm{LMS}}\,\Gamma_{310}\,). \tag{74}$$

Substituting Eqs. (72) and (74) into Eq. (71), and rearranging terms, gives

$$\frac{1-\Gamma_{\mathrm{LMS}}\,\Gamma_{311}}{1-\Gamma_{\mathrm{LMS}}\,\Gamma_{310}}=\frac{b_{111}\,b_{310}}{b_{311}\,b_{110}}+\frac{b_{211}\,b_{301}}{b_{311}\,b_{201}}\ . \tag{75}$$

Since the right side of Eq. (75) is identical to the right side of Eq. (30), the same manipulations may be performed to yield

$$\left|\frac{1-\Gamma_{\mathrm{LMS}}\,\Gamma_{311}}{1-\Gamma_{\mathrm{LMS}}\,\Gamma_{310}}\right|^2=\left(\left|\frac{\dfrac{b_{310}}{b_{110}}}{\dfrac{b_{311}}{b_{111}}}\right|+\left|\frac{\dfrac{b_{301}}{b_{201}}}{\dfrac{b_{311}}{b_{211}}}\right|\right)^2+2\left|\frac{\dfrac{b_{310}}{b_{110}}}{\dfrac{b_{311}}{b_{111}}}\right|\left|\frac{\dfrac{b_{301}}{b_{201}}}{\dfrac{b_{311}}{b_{211}}}\right|(\cos\theta-1)\ . \tag{76}$$

As before, the powers are proportional to the b^2's except for P$_3$, because of the change in Γ_3. Thus

$$P_{311}=\frac{|\,b_{311}\,|^2}{Z_0}\,(1-|\Gamma_{311}|^2)\ , \tag{77}$$

$$P_{310}=\frac{|\,b_{310}\,|^2}{Z_0}\,(1-|\Gamma_{310}|^2\,)\ , \tag{78}$$

and

$$P_{301} = \frac{|b_{301}|^2}{Z_0}(1-|\Gamma_{301}|^2)$$

$$= \frac{|b_{301}|^2}{Z_0}(1-|\Gamma_{310}|^2), \qquad (79)$$

because $\Gamma_{301} = \Gamma_{310}$ has been assumed. The characteristic impedance is denoted by Z_0. Replacing the voltages with powers, gives

$$\left|\frac{1-\Gamma_{\mathrm{LMS}}\,\Gamma_{311}}{1-\Gamma_{\mathrm{LMS}}\,\Gamma_{310}}\right|^2 \frac{(1-|\Gamma_{310}|^2)}{(1-|\Gamma_{311}|^2)} =$$

$$\left[\left(\frac{\dfrac{P_{310}}{P_{110}}}{\dfrac{P_{311}}{P_{111}}}\right)^{1/2} + \left(\frac{\dfrac{P_{301}}{P_{201}}}{\dfrac{P_{311}}{P_{211}}}\right)^{1/2}\right]^2 +$$

$$P_{\mathrm{sq}}(1-\cos\theta), \qquad (80)$$

where

$$P_{\mathrm{sq}} = 2\sqrt{\frac{\dfrac{P_{310}}{P_{110}}}{\dfrac{P_{311}}{P_{111}}} \; \frac{\dfrac{P_{301}}{P_{201}}}{\dfrac{P_{311}}{P_{211}}}}\;. \qquad (81)$$

As in Appendix A, using the argument that the function is minimum when the angle is 0, and substituting in the proportional readings

$$C^2_{\mathrm{HL}}\left|\frac{1-\Gamma_{\mathrm{LMS}}\,\Gamma_{311}}{1-\Gamma_{\mathrm{LMS}}\,\Gamma_{310}}\right|^2 \frac{(1-|\Gamma_{310}|^2)}{(1-|\Gamma_{311}|^2)} =$$

$$\left[\left(\frac{\dfrac{P_{310}}{P_{110}}}{\dfrac{P_{311}}{P_{111}}}\right)^{1/2} + \left(\frac{\dfrac{P_{301}}{P_{201}}}{\dfrac{P_{311}}{P_{211}}}\right)^{1/2}\right]^2. \qquad (82)$$

Acknowledgments

The authors acknowledge the contributions of C. Allred, who originally developed the theoretical analysis of the linear measurement system; F. Marler, who designed the 30 MHz LMS prototype; J. Juroshek and P. Leyva for reviewing this paper; P. Voris and K. Talley who helped assemble the LMS; G. Rebuldela for his advice throughout the project; and N. Larsen for supplying the data found in Fig. 4.

12. References

[1] R. A. Ginley and C. M. Allred, 1.25 MHz Attenuation Measurement System, IEEE Trans. Instrum. Meas. **IM-35**, 463-466 (1986).
[2] N. T. Larsen, A New Self-Balancing DC-Substitution RF Power Meter, IEEE Trans. Instrum. Meas. **IM-25**, 343-347 (1976).
[3] F. R. Clague, Power Measurement System for 1 mW at 1 GHz, Natl. Inst. Stand. Technol., Technical Note 1345 (1990).
[4] Taylor, B. N. and Kuyatt C. E., Guidelines for Evaluating and Expressing the Uncertainty of NIST Measurement Results, Natl. Inst. Stand. Technol., Technical Note 1297 (1993).

About the authors: *Jeffrey A. Jargon is an electrical engineer and a member of the NIST Microwave Metrology Group, where his main responsibilities are in cw, coaxial high power and 30 MHz attenuation measurements. Ronald A. Ginley is an electrical engineer in the Microwave Metrology Group. His responsibilities include the design of dual six-port systems, and software, hardware, and technical support for the 1.25 MHz Attenuation Measurement System and the lower frequency six-port systems. Douglas D. Sutton was a physical science technician in the Microwave Technology Group when this work was done. The National Institute of Standards and Technology is an agency of the Technology Administration, U.S. Department of Commerce.*